Available online at www.sciencedirect.com

jmr&t Journal of Materials Research and Technology

www.jmrt.com.br

Review Article

Fundamental aspects of the martensite transformation curve in Fe-Ni-X and Fe-C alloys

José Roberto Costa Guimarães[a,b], *Paulo Rangel Rios*[a,*]

[a] *Universidade Federal Fluminense, Escola de Engenharia Industrial Metalúrgica de Volta Redonda, Av. dos Trabalhadores, 420, Volta Redonda, RJ 27255-125, Brazil*

[b] *Mal. Moura 338H/22C, São Paulo, SP 05641-000, Brazil*

ARTICLE INFO

Article history:
Received 16 January 2018
Accepted 25 April 2018
Available online 28 May 2018

Keywords:
Martensitic transformations
Microstructure modeling
Phase transformations
Steels
Fe-Ni-X alloys

ABSTRACT

This work initially reviews fundamental aspects of nucleation and growth of martensite. Next, based on previous work as well as on new unpublished work it proposes a probabilistic formalism to describe/analyze the martensite transformation curves. Furthermore, it discusses the autocatalysis that modulates the advance of martensite's nucleation determined by the stability of the alloy-system. The accommodation of the transformation strains that gives the volume fraction transformed refers to (local) interactions among growing units as well with the austenite matrix. The scarcity/randomness of martensite nucleation loci in the austenite, which promotes the initially scattered transformation, as well as underlies the microstructural evolution. The formalism was validated by fitting the transformation curves typical of the athermal as well as of the thermal-activated martensites.

José Roberto Costa Guimarães obtained his Ph.D. in Stanford in 1969. He was a Professor at Military Institute of Engineering. He left to join Companhia Brasileira de Metalurgia e Mineração where he worked until his retirement. He is now an external colaborator with Universidade Federal Fluminense and is also a Private Consultant. He won the Hubertus Colpaert medal from ABM.

Paulo Rangel Rios obtained his undergraduate and M.Sc. degree in Metallurgical Engineering at Instituto Militar de Engenharia in Rio de Janeiro. In 1986 he obtained his Ph.D. in Metallurgy and Materials Science from the University of Cambridge where he studied under Professor R.W.K. Honeycombe. He was a visiting Professor at University of Tokyo in 1998 and at University of Aachen in 2000 and 2009/2010 working with Professor Günther Gottstein. He obtained the Humboldt Research award in 2009. Since 1994 he is Professor Titular (full Professor) at Universidade Federal Fluminense, Escola de Engenharia Industrial Metalúrgica de Volta Redonda.

He is a member of ABM and one of the Editors of Journal of Materials Research and Technology.

* *Corresponding author.*

https://doi.org/10.1016/j.jmrt.2018.04.007

1. Introduction

The term "martensite" was introduced in 1895, by the French metallographer F. Osmond [1] who coined the name to recognize the early support by the German metallurgist A. Martens to metallographic investigations. Since then, practical and fundamental aspects of martensite have been a continuing endeavor of metallurgists, aiming to improve performance and broaden steels utilization. Nowadays, steels bear optimized microstructures, which frequently derive from the response of martensite transformation to mechanical stimuli.

The early investigators established the relationship between the composition of the steel, the martensite fraction transformed, and the martensite morphology. The nearly supersonic formation of martensite during continuous cooling [2] entailed perception that the transformation proceeded by the nucleation of several units instead of the growth of a few ones. Until the 1950s when Kurdjumov and Maximova [3,4] described "isothermal" martensite, the transformation was generally considered "athermal" (not thermally activated). Thereafter, classical and non-classical concepts have been proposed to rationalize martensite's kinetic behaviors [5,6]. Compositional [7] as well as structural heterogeneities [8] were considered to explain the nucleation-controlled aspect of martensite. Meantime, advances in the analysis of martensite's crystallography [9] suggested a semi-coherent martensite–austenite interface [10], which renders improbable the martensite propagation by single-domain nuclei crossing a classical nucleation path. Then, the critical step in the martensite propagation was operationally relocated from austenite→martensite to "embryo"→martensite, where embryo meant a pre-transformation assemble.

Despite the relative success of this conceptualization [5], the fact that the assumed volumetric embryonic features could not be observed led to the fault model advanced by Olson [11]. This model postulates the dissociation of an austenite defect into a martensite embryonic fault-assemble whose propagation depends on the mobility of its interfacial structure [12–15]. The presence of long-range stress fields promotes athermal drag, whereas short-range interactions promoted by the interfacial core may be overcome by thermal activation [16,17], explaining martensite's "athermal" and "isothermal" kinetics. The dynamic aspects of the fast growth of martensite have been considered by Meyers [18]. Meyers proposed that the highly compressed state resultant from the nearly instantaneous formation of a martensite nucleus entails a longitudinal wave that generates the midrib as well as activates a transverse wave that completes the transformation of austenite into martensite.

Pursuing different venues, Chen et al. [19] associated the martensite transformation path with the austenite conversion into a sequence of domains transformed by complementary lattice correspondence (Bain strain). Kakeshita et al. [20–22] introduced a probabilistic approach to describe time-dependent as well as to time-independent martensite kinetic if the transformation takes place when excited austenitic nano-clusters cross the reaction path. More recently, the simulation of heterogeneous martensite nucleation due to Zhang et al. [23] reiterated the view that martensite nucleates from multi-domains ensembles in the volume of influence of austenite defects. Indeed, martensite embryonic-domains may be stabilized by the relaxation of the lattice correspondence misfit in a grain boundary environment [24]. Related results of Monte Carlo quench experiments [25,26] suggest entropic barriers on martensite transformation path, a topic also considered in [27].

In the present work, we describe a probabilistic approach to the martensite transformation curve that conforms to the view that the resultant microstructure is shaped by the local conditions [28] coherently with the diffusionless-displacive aspect of the transformation initiated at scarce and randomly disperse austenitic loci [29].

2. Microstructural evolution

At present it is accepted that "a martensitic transformation is a shear-dominant, lattice-distortive, diffusionless transformation occurring by nucleation and growth" [30]. As consequence of these specificities, a martensite unit cannot grow through high-angle boundaries so that the growth is frequently halted by impingement. Thus, martensite's shape-strain must be locally relaxed into the austenite or by sympathetic nucleation events.

The crystallographic bias (variant-selection) introduced by the latter events are evidenced by the zigzagging martensite units seen in Fig. 1, as well as by the packets and the blocks typical of other martensite microstructures [31]. Here, we share the view that the martensite transformation modulated by autocatalysis, is driven by the effect of the external variable on the stability of the system. However, the intensity of the transformation (the volume fraction transformed) depends on the local interactions among the martensite units as well as with the austenite matrix.

3. Formal description of the microstructure

Historically, the advance of the martensite transformation in iron base alloys has been described by transformation-curves that give the volume fraction of material transformed into martensite as a function of the external variable, e.g., the quenching temperature. Stereology teaches us that the volume fraction of a material feature is given by the product of the number density times the mean volume of the features

$$V_V = \upsilon N_V \tag{1}$$

In the case of martensite, we substitute υ_M for υ, N_{VM} for N_V, V_{VM} for V_V. Thus, υ_M stands for the *overall* mean volume of a martensite unit in the material. However, the experiments of Cech and Turnbull [29] have shown that Fe-30wt%Ni particulate does not transform uniformly, suggesting the existence of scarce/random-distributed number of defects that catalyze the heterogeneous martensite transformation. Thus, the transformation curve bears this probabilistic aspect of the transformation. Moreover, it should be apparent that the (local) volume fraction of martensite in a transformed grain is generally distinct from the (overall) material fraction transformed. Cohen and Olson [32] derived a mathematical

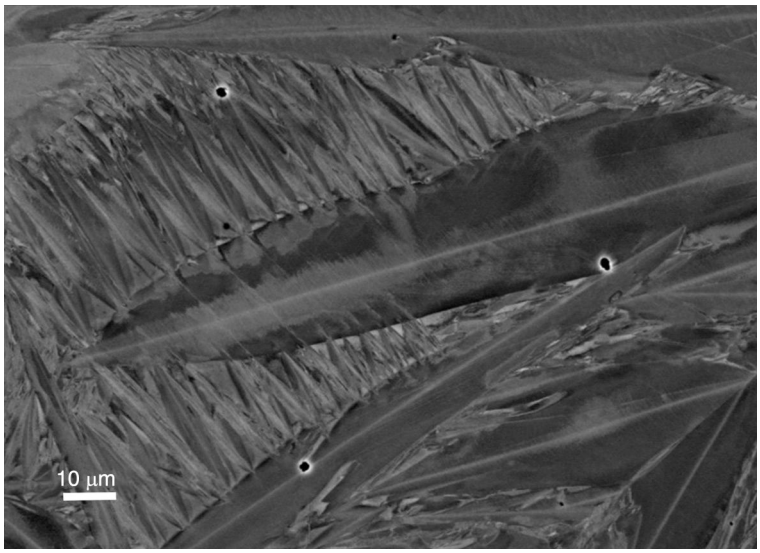

Fig. 1 – Fe-31wt%Ni-0.02wt%C transformed by cooling to boiling liquid nitrogen. Observe the effect of "zigzag" of the plates that is caused by stress accommodation.
Courtesy of Dr. K. Zilnyk.

expression to describe the results of Cech and Turnbull on a system consisting of particles, not a polycrystal. Cohen and Olson [32] considered that the mean number of nucleation loci per particle: $q_p n_V^T$ was given by the product of the mean particle volume, q_p, times the number of nucleation loci per unit of volume, n_V^T. Cohen and Olson [32] used the Poisson distribution to model the number of nucleation loci per particle. So, the probability that a particle contains "n" nucleation loci is given by Poisson distribution $P(n) = \frac{(q_p n_V^T)^n}{n!} e^{-(q_p n_V^T)}$. Therefore, the probability that a particle contains no nucleation loci is given by $P(n=0) = \frac{(q_p n_V^T)^0}{0!} e^{-(q_p n_V^T)} = e^{-(q_p n_V^T)}$. Thus, the probability that a particle contains at least one nucleation locus is simply $P_p = 1 - P(n=0)$. Finally, we recover the result of Cohen and Olson [32]: the probability that a particle contains at least one nucleation locus at temperature T

$$P_p = 1 - \exp(-q_p n_V^T) \tag{2}$$

where n_V^T is the number density of preexisting nucleation loci, and q_p is the mean particle volume. Tantamount, Eq. (2) gives the volume fraction of material comprising the particles where martensite formed. In bulk polycrystalline material of similar composition, Fe-31wt%Ni-0.02wt%C, clusters of partially transformed grains form due to intergrain interactions [33], see Fig. 2. The phase-field model described in Ref. [25] suggest that although Fe-31wt%Ni martensite may nucleate at grain boundaries, the intragrain growth is a cooperative event between units with complementary crystallographic variants that can develop into a chain-reaction. Furthermore, since such a cooperative event is also possible between adjacent grains, the initial chain-reaction may reach neighboring grains and burst into clusters of transformed grains [34–37]. Recalling Magee [38], it is admissible that grains are equally transformed by the chain-reactions, so that the number density of transformed grains at temperature $T \leq M_s$ is given by the ratio N_{VM}/β, where β is the average number of martensite units per transformed grain. Thus, recognizing the randomness of the initial nucleation loci, we substitute the volume fraction of material comprising partially transformed grains, V_{VG}, by the probability of finding at least one of them

$$V_{VG} = 1 - \exp(-qN_{VM}/\beta) \tag{3}$$

where q is the mean austenite grain volume. This Eq. (3) is analogous to the heuristic equation introduced in Ref. [33]. Proceeding, note that the volume fraction of martensite in these autocatalytic transformed grains is $f = \beta v_{MG}/q$, where v_{MG} is the local martensite mean unit volume modulated by the autocatalysis. Thus, the probability of finding martensite in the material is given by $f \cdot qN_{VM}/\beta = v_{MG}N_{VM}$. Therefore, in a material that conforms to the above rules, the overall martensite volume fraction may be expressed as

$$V_{VM} = 1 - \exp(-v_{MG}N_{VM}) \tag{4}$$

Noteworthy, Eq. (4) refers to the influence of autocatalysis instead to the size of austenite compartments as in Fisher's partition equation [7].

4. Transformation curve

The search for an optimum equation for martensite's transformation curve has been a continuing endeavor in materials R&D [38–53]. Among the ones advanced, the empirical equation due to Koistinen and Marburger [40]

$$V_{VM} = 1 - \exp(-\alpha(M_s - T)) \tag{5}$$

where $\alpha \approx 0.011$, M_S is the martensite start temperature and T is the quench-temperature, became the one most operationally used and/or mentioned in the literature.

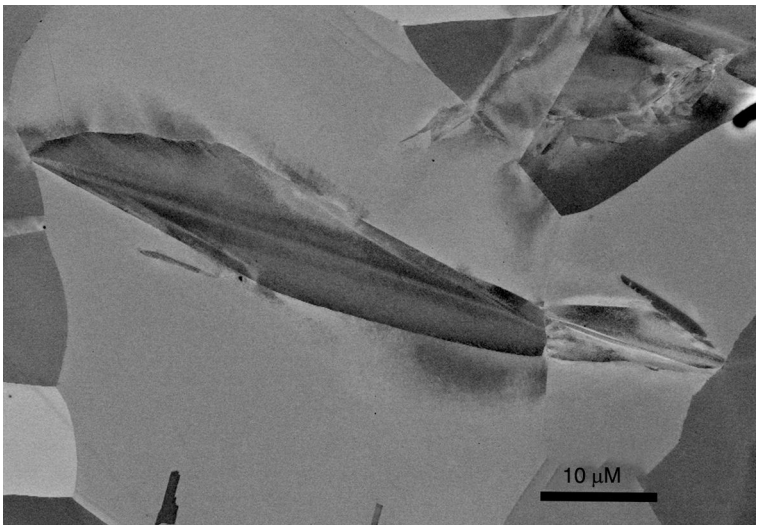

Fig. 2 – Scanning electron micrograph using backscattered electrons of Fe-31wt%Ni-0.02wt%C transformed at the martensite start temperature. One martensite plate partitions the grain and hits the grain boundary inducing the formation of another plate located within a neighbor grain. Because of this intergrain autocatalysis clusters of partially transformed grains may result.
Courtesy of Dr. K. Zilnyk.

Meantime, the influence of the microstructure on the transformation curve has been established [41,44,45] and modifications have been proposed to Eq. (5) based upon the system properties.

Here, we revisit the modeling of the transformation curve. We start by focusing the admittedly nucleation-controlled, autocatalytic and athermal martensite transformation in quenched Fe-31wt%Ni-0.02wt%C. Thus, we suppose that an incremental variation in the external variable [48] (e.g., the quench temperature) results in an increment in the number of martensite units observed in the microstructure, and admitting that the chemical driving-force is linearly dependent on the temperature,

$$dN_{VM} = \varphi_k N_{VM}\left(\frac{-dT}{T^* - T}\right) \tag{6}$$

where φ_k is a kinetic-factor. T^* is the highest temperature at which an austenite defect is able to sustain correlated atomic groups in the presence of thermal agitation. The integration of Eq. (6) between the martensite start temperature, M_s, and the quench temperature, T, gives

$$N_{VM} = N_{VM0}\left(\frac{T^* - T}{T^* - M_s}\right)^{\varphi_k} \tag{7}$$

where N_{VM0} is the number density of martensite units transformed at the M_s temperature. Therefore, substituting Eq. (7) into Eq. (4), and admitting that at $T = M_s$, the local fraction transformed is $V_{VM0} = v_{MG}N_{VM0}$, gives the equation of the athermal transformation curve.

$$V_{VM} = 1 - \exp\left(-V_{VM0}\left(\frac{T^* - T}{T^* - M_s}\right)^{\varphi_k}\right) \tag{8}$$

It can be shown that the analog of Eq. (8) relevant to a thermally activated, time-dependent ("isothermal") martensite transformation at temperature T is

$$V_{VM} = 1 - \exp\left(-V_{VM0}\left(\frac{t - \tau}{t_0 - \tau}\right)^{\varphi_k^T}\right) \tag{9}$$

where τ is the incubation-time and t_0 is the detectable initial transformation time. V_{VM0} is the volume fraction transformed at t_0 in a grain. The temperature-dependence in the kinetic-factor is indicated in the superscript index, φ_k^T.

At this point, it is appropriate recalling that the utilization of probabilistic concepts to describe/analyze aspects of martensitic transformations is not new [20,32]. The model's Eqs. (8) and (9) were checked by fitting experimental data. Nevertheless, likewise the models/equations referred in our review, ours bears simplifications, e.g. Eq. (6), whereas the probabilistic underlay consolidated in Eq. (4) is an expeditious alternative to deal with the complex size-distribution of the martensite units [7,53].

4.1. *Athermal transformation*

The fittings of Eq. (8) to the transformation-curves of Fe-31wt%Ni-0.02wt%C with different grain-sizes (0.027–0.142 mm) transformed by quenching, and those of the dilatometer-transformed Fe-C steels [42] are shown in Figs. 3 and 4, respectively. The values of the fitting parameters are depicted in Table 1. The values of $T^* \geq M_s$ refer to the chemistry of the alloy's chemistry. In case of barrierless transformation, once an austenite defect sustains a correlated atomic group, and the available driving force suffices to take the transformation elastic energy, "*athermal*" propagation occurs. The sharp differences between the values of V_{VM0} (Fe-Ni-C/Fe-C) are coherent with the bursting aspect of the Fe-Ni-C martensite. In the Fe-Ni-C, which transforms below room temperature into lenticular-twinned-martensite,

Table 1 – Fitting parameters – Eq. (8).

	Fe-31Ni-0.02C0.027 mm	Fe-31Ni-0.02C0.048 mm	Fe-31Ni-0.02C0.142 mm	Fe-0.46C	Fe-0.66C	Fe-0.80C
T^* (K)	213	221	227	587	535.7	503
M_S (K)	212	220	220	586	535.5	502
φ_k^T	0.76	0.60	0.85	1.17	1.13	1.17
V_{VM0}	0.02	0.07	0.30	0.003	0.002	0.006
R^2	0.92	0.91	0.94	0.99	0.99	0.99

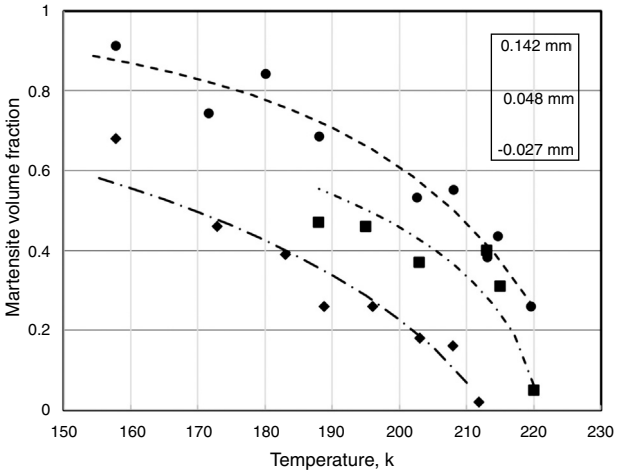

Fig. 3 – Fe-31wt%Ni-0.02wt%C – fittings of transformation-curves with Eq. (8).

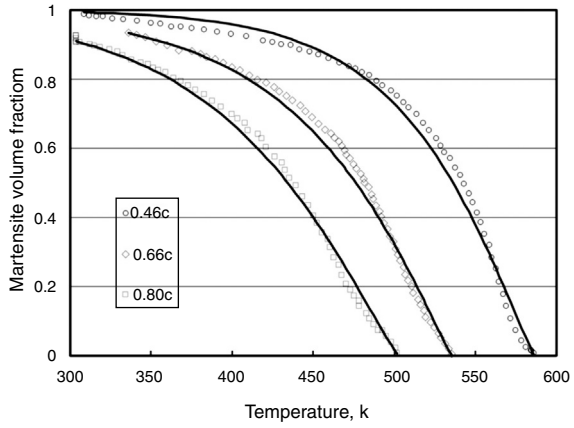

Fig. 4 – Best fit of the transformation-curves of Fe-0.46wt%C, Fe-0.66wt%C, and Fe-0.80wt%C with Eq. (8). Data from Ref. [42].

φ_k is located within the interval [0.76–0.85]. By contrast, Fe-C steels transform at or above room temperature into smaller lath, dislocated-martensite, which generally do not gauge the austenite. For Fe-C steels φ_k is located within the interval [0.94–1.17]. That is more laths then lenses are necessary to yield the same martensite volume fraction what corroborates that the shape-strain relaxation (autocatalysis and/or slip) influences the progress of martensite transformation.

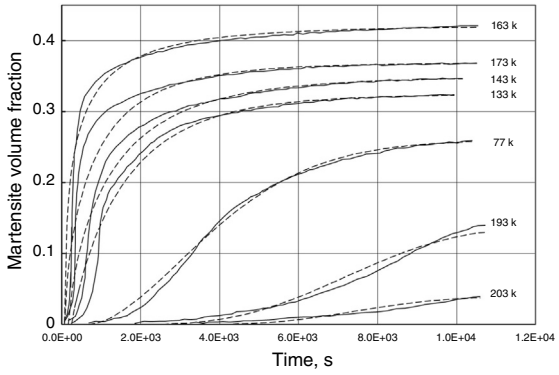

Fig. 5 – Best fit of Fe-23.2wt%Ni-2.8wt%Mn-0.009wt%C transformation-curves with Eq. (9). Data from Ref. [54].

Table 2 – Best fit parameters – Eq. (9).

T, K	τ, s	φ_k^T	V_{VM0}	R^2
77	41.4×10^3	1.7	8.06E−07	0.96
133	14.4×10^3	0.88	1.72E−03	0.98
143	10.4×10^3	0.74	5.39E−03	0.98
163	4.7×10^3	0.48	6.04E−02	0.98
173	4.6×10^3	0.69	1.03E−02	0.95
193	111.6×10^3	2.8	2.39E−11	0.65
203	204.4×10^3	2.8	5.14E−11	0.83

4.2. *Isothermal transformation*

The data set typical of isothermal martensite transformation in Fe-23.2wt%Ni-2.8wt%Mn-0.009wt%C used in the present work was issued by Ghosh and Raghavan [54]. These data were incorporated here by scanning and digitizing the charts in Fig. 2 in their paper. The capability of Eq. (9) to describe the transformation curves is evident in Fig. 5. The fittings are better at the larger fractions transformed. Since the original charts did not permit to distinguish τ from t_0, we assumed $\tau/t_0 = 0.9999$, noting that the quality of the fittings was not impaired by using a smaller τ/t_0 ratio, e.g. 0.80. The fitted values of V_{VM0}, τ, and φ_k^T, as well as the respective fitting-correlations are depicted in Table 2. Perusing this table, it is conspicuous that the fitting parameters go through maximum/minimum values about the same intermediate temperature: ~160 K. In the case of the isothermal martensite, the nucleation is thermally activated. That is, although the population of correlated atomic groups available to cross the transformation path [55] may be stabilized by decreasing the temperature, their ability to overcome the barrier is impaired. Accordingly, the values of τ and φ_k^T delineate C-curves – see Figs. 6 and 7. The ultimate temperature at which an austenite

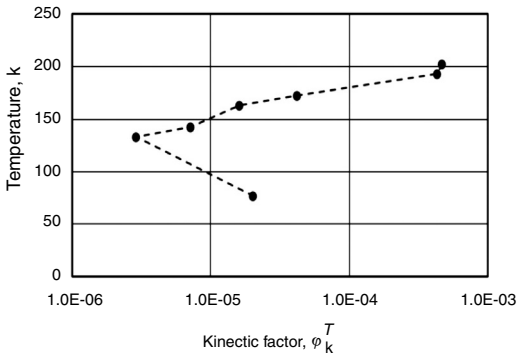

Fig. 6 – Fe-23.2wt%Ni-2.8wt%Mn-0.009wt%C data: temperature variation of the kinetic-factor – refer to Eqs. (3) and (9).

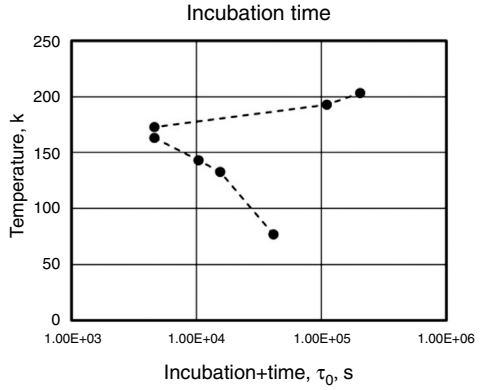

Fig. 7 – Fe-23.2wt%Ni-2.8wt%Mn-0.009wt%C – temperature variation of the incubation time, τ, s – refer to Eq. (9).

defect is able to sustain correlated atomic groups in face of thermal agitation, T*, sets the upper limit for the C-curves.

The apparent activation-energy obtained from the upper limbs of the C-curves 2.7×10^{-20} J/event and 4.9×10^{-20} J/event compare with values for the activation energy for martensite nucleation reported Ref. [54].

The parameter τ refers to the activation energy typical of the initial martensite nucleation, ΔWa. Recalling that the martensite transformation in particulate Fe-30wt%Ni [29] warrant expressing the probability of existing operational nucleation loci in the austenite by the ratio $\frac{\Delta S(T*-T)}{k_B T}$, where ΔS is the martensite transformation entropy, T^* was above defined, k_B is Boltzmann's constant, and T is the reaction temperature [54], we write

$$\tau^{-1} = \vartheta \Delta S \left(\frac{T* - T}{k_B T}\right) \exp\left(-\frac{\Delta Wa}{k_B T}\right) \quad (10)$$

where ϑ is a frequency factor that depends on the nucleation mechanism [54]. In Fig. 8 we compare the values of ΔWa reported in Ref. [54] with the values now calculated by inputting the values of τ from Table 2 into Eq. (10). Note that fitting $T^* = 206$ K, and $\vartheta = 10^{13}$ s^{-1} as in [54], the charts converge. Remarkable, the convergence hints that the *local* austenite stability is influenced by thermal agitation.

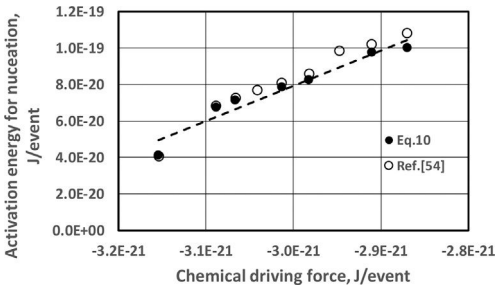

Fig. 8 – Fe-23.2wt%Ni-2.8wt%M-0.009wt%C – activation energy for martensite nucleation as a function of the chemical driving force: ● – calculated with Eq. (10), ○ – reported in Ref. [54].

5. Autocatalysis and intergrain-spread in athermal martensite

Here we consider this subject by referring to the microstructure evolution in quench-transformed Fe-31wt%Ni-0.02 wt% whose martensite units gauge (partition) the austenite grains. As mentioned, martensite's shape-strain is locally relaxed by slip [56,57] as well as by sympathetic nucleation [35]. The latter yields chain-reactions forming zigzags modulated by variant selection that feedback strain-energy. Frequently, this process entails a fast, near explosive, transformation that spreads into adjacent grains forming clusters of transformed grains. The impingement of austenite-gauging martensite units on grain boundaries is critical for cluster formation [58].

This intergrain spread of the martensite transformation in Fe-31wt%Ni-0.02 wt% has been characterized by metallographic analysis. The area density of the ordinary grain boundaries that delineate the clusters of transformed grains, S_{VG}, and the contained volume fraction of material (austenite plus martensite), V_{VG}, were determined as described in Ref. [59]. The intergrain transformation does not visibly affect the austenite grain boundaries. However, the size of the clusters is delimited by some drag effect or by coalesce on adjoining. The latter is evidenced by the fact that S_{VG} reaches a maximum at an intermediate value of V_{VG} [33]. Henceforth, to characterize the drag effect on the clusters' growth we calculated their "coalescence-compensated" volume [60]

$$Q_c = \left(\frac{\phi(1 - V_{VG}) \ln (1 - V_{VG})^{-1}}{S_{VG}}\right)^3 \quad (11)$$

where ϕ is a shape factor. The values of Q_C, assuming tetrakaidecahedra clusters and grains ($\phi = 16/3$) are shown in Fig. 9, along with the values of the parameter β, which refers to the intragrain autocatalytic transformation. The values of β were calculated with Eq. (3). Observe that β is nearly invariant, coherently with the mechanical (athermal) feedback provided by the variant-selection in the zigzags [35]. On the other hand, the values of Q_C fit the Arrhenius equation. Despite the impaired fitting-correlations ($R^2 = 0.76$–0.37) due to the hardship to delineate the clusters in fine grained materials, the obtained apparent activation-energies, 2.0×10^{-20} J/event – 2.4×10^{-20} J/event compare with

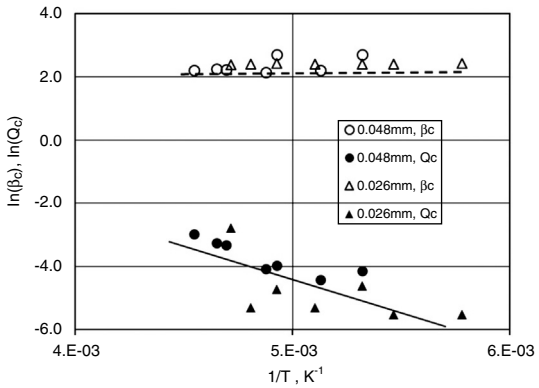

Fig. 9 – Fe-31wt%Ni-0.02wt%C – evidence of thermally activated process step on intergrain spread. Arrhenius plots of Q values, mean intercept length: ● −0.048 mm and ▲ −0.027 mm, from Tables 1 and 2. Apparent activation energies 2.8 × 10^{-20} J/event. The values of β, mean intercept length: ○ −0.048 mm and △ −0.027 mm, are also shown. Data from Ref. [59].

the activation energies for the nucleation of martensite in a similar Fe-Ni-C alloy subject to micro-seconds tensile stress-pulses, 4.1×10^{-20} J/event – 6.3×10^{-20} J/event, attributed to nucleation controlled by interface-mobility [61]. Nonetheless, since the parameter β, which characterizes the intragrain-spread of the transformation, is temperature-independent. It is apparent that the temperature dependence in the intergrain-spread must relate to a distinct thermally activated process. In any case, the thermally activated aspect of the martensite autocatalysis in the "athermal" Fe-Ni-C goes along with a temperature dependent kinetic-factor in the Fe-Ni-Mn.

6. Summary and conclusions

This work addressed the description and analysis of the martensite transformation curves, bearing a survey of literature of the present understanding about this matter. The work comprised a probabilistic description of microstructure evolution preceded the derivation of the equation of the transformation. The latter assumed that an increment in the number of martensite units refers to an incremental variation in the external variable modulated by the autocatalysis.

The following concepts underlie the model. (i) The advance of nucleation-controlled martensite propagation is determined by the stability of the alloy-system, modulated by the autocatalysis. (ii) The volume fraction transformed depends on the local interactions in the grains, between a growing unit, their neighbors and the austenite matrix. (iii) The initial, scattered and heterogeneous propagation of martensite, sets the base for the distribution of the martensite in the material and for the microstructural evolution. (iv) The parameters in the derived equations refer to the kinetic aspects of the transformation.

The formalisms were validated by fitting experimental transformation curves typical of the athermal as well as of the thermal-activated martensitic transformations. The values of the fitting parameters were compared with previous, independent, results described in the literature. The following is noteworthy:

The probabilistic description of the relationship between the volume fraction and the number of units transformed constitutes an expeditious as well as an operational alternative to considering the size-distribution of the martensite units.
The values of the parameters characteristic of the "isothermal" (thermally activated) transformation data support the view that martensite nucleation initiates in the volume of influence of austenite defects, if they sustain a correlated atomic group in face of thermal agitation. Tantamount, thermal agitation influences in the *local* austenite stability.
The analyzed transformation-curves suggest that the relaxation of the shape-change either by autocatalysis feedback, by the austenite plasticity or by assimilation into the martensite has a determinant effect in the volume fraction transformed, thence in the transformation curve.

Conflicts of interest

The authors declare no conflicts of interest.

Acknowledgements

P.R. Rios, is grateful to Conselho Nacional de Desenvolvimento Científico e Tecnológico, CNPq, and to Fundação de Amparo à Pesquisa do Estado do Rio de Janeiro, FAPERJ, for financial support. The authors are grateful to Prof. Kahl Zilnyk for providing the micrographs used in Figs. 1 and 2.

REFERENCES

[1] Osmond MF. Méthode Générale pour l'analyse micrographique des acier ao carbone. Bulletin de la Société d'Encouragement pour lÍndustrie Nationals 1895;10:465–93.
[2] Bunshah RF, Mehl RF. Rate of propagation of martensite. Trans AIME 1953;197:1251–8.
[3] Kurdjumov GV, Maximova OP. Kinetics of austenite to martensite transformation at low temperatures. Dokl Akad Nauk SSSR 1948;61:83.
[4] Kurdjumov GV, Maximova OP. The question of the energy of formation of the nuclei of martensite. Dokl Akad Nauk SSSR 1950;73:95.
[5] Kaufman L, Cohen M. Thermodynamics and kinetics of martensitic transformations. Prog Metal Phys 1958;7:165–246.
[6] Olson GB, Cohen M. Principles of martensitic transformation, frontiers in materials technologies. Amsterdam: Elsevier; 1985. p. 43.
[7] Fisher JC, Hollomon JH, Turnbull D. Kinetics of the austenite–martensite transformation. Trans AIME 1949;85:691–770.
[8] Cohen M, Machlin ES, Paranjpe VG. Thermodynamics in physical metallurgy. American Society for Metals; 1949. p. 242–65.
[9] Wechsler MS, Lieberman DS, Read TA. On the theory of the formation of martensite. Trans AIME 1953;197:1503–15.
[10] Knapp H, Dehlinger U. Mechanik und kinetik der diffusionslosen martensitbildung Dynamique et cinetique

de la transformation martensitique sans diffusion. Acta Metall 1956;4:289–97.
[11] Olson GB (Sc.D. Thesis) A general mechanism of martensitic nucleation. MIT; 1974.
[12] Olson GB, Cohen M. A general mechanism of martensitic nucleation: Part I. General concepts and the FCC->HCP transformation. Metall Trans A 1976;7A:1897–904.
[13] Olson GB, Cohen M. A general mechanism of martensitic nucleation: Part II. FCC-> BCC and other martensitic transformations. Metall Trans A 1976;7A:1905–13.
[14] Olson GB, Cohen M. A general mechanism of martensitic nucleation: Part III. Kinetics of martensitic nucleation. Metall Trans A 1982;7A:1905–13.
[15] Olson GB, Cohen M. Theory of martensitic nucleation: a current assessment. In: Aaronson HI, Laughlin DE, Skerka RF, Wayman CM, editors. Proceedings of an international conference on solid–solid phase transformations, TMS-AIME. Warrendale, Pennsylvania, USA; 2010. p. 1245.
[16] Ghosh G, Olson GB. Kinetics of FCC-BCC heterogeneous martensitic nucleation – I: the critical driving force for athermal nucleation. Acta Mater 1994;42:3361–70.
[17] Ghosh G, Olson GB. Kinetics of FCC-BCC heterogeneous martensitic nucleation – II: thermal activation. Acta Metall 1994;42:3371–9.
[18] Meyers MA. On the growth of lenticular martensite. Acta Metall 1980;28:757–70.
[19] Chen S, Khachaturyan AG, Morris JW Jr. Computer simulation of the martensite transformation in a model two-dimensional body. In: Owen WS, editor. Proceedings of ICOMAT-79. Cambridge, MA: MIT Press; 1979. p. 94–9.
[20] Kakeshita T, Kuroiwa K, Shimizu K, Ikeda T, Yamagishi A, Date M. A new model explainable for both the athermal and isothermal natures of martensitic transformations in Fe-Ni-Mn alloys. Trans Jpn Inst Met 1993;34:423–8.
[21] Kakeshita T, Shimizu K. Effects of hydrostatic pressure on martensitic transformations. Mater Trans JIM 1997;38:668–81.
[22] Kakeshita T, Fukuda T, Saburi T. Time-dependent nature and origin of displacive transformation. Sci Technol Adv Mater 2000;1:63–72.
[23] Zhang W, Jin YM, Khachaturyan AG. Phase field microelasticity modeling of heterogeneous nucleation and growth in martensitic alloys. Acta Mater 2007;55:565–74.
[24] Heo W, Chen L-Q. Phase-field modeling of displacive phase transformations in elastically anisotropic and inhomogeneous polycrystals. Acta Mater 2014;76:68–81.
[25] Shankaraiah N, Murthy KPN, Lookman T, Shenov SR. Incubation times and entropy barriers in martensitic kinetics: Monte Carlo quench simulation of strain pseudospins. Europhys Lett 2010;92:36002.
[26] Shankaraiah N. Monte Carlo simulations of vector pseudospins for strains: microstructures and martensitic conversion times. J Alloys Compd 2015;675:211–22.
[27] Kastner O, Shneck RZ. On the entropic barrier in a martensitic transformation. Philos Mag 2015;95:1282–308.
[28] Kastner O, Ackland GJ. Mesoscale kinetics produces martensitic microstructure. J Mech Phys Solids 2009;57:109–21.
[29] Cech RE, Turnbull D. Heterogeneous nucleation of the martensite transformation. Trans AIME 1956;206:124–32.
[30] Christian JW, Olson GB, Cohen M. Classification of displacive transformations: what is a martensitic transformation? Journal de Physique IV, Colloque C8, supplément au Journal de Physique III 1995;5:3–10.
[31] Maki T. Recent advances in understanding martensite in steels. In: Furuhara T, Tsuzaki K, editors. Proceedings of the 1st international symposium on steel science. Tokyo, Japan: ISIJ; 2007. p. 1–10.
[32] Cohen M, Olson GB. Martensite nucleation and the role of the nucleating defect. Suppl Trans JIM 1976;17:93–8.
[33] Guimarães JRC, Saavedra A. A computer-assisted analysis of the spread of martensite-transformation. Mater Sci Eng 1984;62:11–5.
[34] Raghavan V, Entwisle AR. Isothermal mechanism kinetics in iron alloys. The physical properties of martensite and bainite. Special report, vol. 93. Iron and Steel Institute; 1965. p. 29–37.
[35] Bokros JC, Parker ER. The mechanism of the martensite burst transformation in Fe-Ni single crystals. Acta Metall 1963;11:1291–301.
[36] Entwisle AR, Feeney JA. The mechanism of phase transformation in crystalline solids. Inst Met Monogr 1969;33:156–61.
[37] Entwisle AR. The kinetics of martensite formation in steels. Metall Trans 1971;2:2397–407.
[38] Magee CL. The nucleation of martensite. In: Aaronson HI, editor. Phase transformations. ASM; 1968. p. 115–56.
[39] Harris WJ, Cohen M. Stabilization of the austenite–martensite transformation. Trans AIME 1949;180:447–70.
[40] Koistinen DP, Marburger RE. A general equation prescribing the extent of the austenite–martensite transformation in pure iron-carbon alloys and plain carbon steels. Acta Metall 1959;7:59–60.
[41] Van Bohemen SMC, Sietsma J. Effect of composition on kinetics of athermal martensite formation in plain carbon steels. Mater Sci Technol 2009;25:1009–12.
[42] Van Bohemen SMC, Sietsma J. Martensite formation partially and fully austenitic plain carbon steels. Metall Mater Trans A 2009;40A:1059–68.
[43] Lee SJ, van Tyne CJ. A kinetics model for martensite transformation in plain carbon and low-alloyed steels. Metall Mater Trans A 2012;43A:422–7.
[44] Lee S-J, Lee S, De Cooman BC. Martensite transformation of sub-micron retained austenite in ultra-fine-grained manganese transformation-induced plasticity steel. Int J Mater Res 2013;104:423–9, http://dx.doi.org/10.3139/146.110882.
[45] Guimarães JRC, Rios PR. Driving force and thermal activation in martensite kinetics. Metall Mater Trans A 2009;40:2255–509.
[46] Guimarães JRC, Rios PR. Modeling lath martensite transformation curve. Metall Mater Trans A 2013;44:2–4.
[47] Guimarães JRC, Rios PR. Microstructural analysis of the martensite volume fraction. Metall Mater Trans A 2013;44:147–51.
[48] Huyan F, Hedström P, Borgenstam A. Modelling of the fraction of martensite in low-alloy steels. International conference on martensitic transformations, ICOMAT-2014. Mater Today Proc 2015;2 (Suppl. 3):S561–4.
[49] Fukuda T, Kakeshita T, Lee Y. An interpretation of martensitic transformation in a Ni45Co5Mn3.6In13.5 alloy. Acta Mater 2014;81:121–7.
[50] Hong M, Wang K, Chen Y, Liu F. A thermo-kinetic model for martensitic transformation kinetics in low-alloy steels. J Alloys Compd 2015;647:763–7.
[51] Liu C, Shao Y, Chen J, Liu Y. Non-instantaneous growth characteristics of martensitic transformation in high Cr ferritic creep-resistant steel. Appl Phys A 2016;122:715.
[52] Chen WYC, Winchell PG. Martensite plate arrangement in O1 tool steel. Metall Trans A 1976;7A:1177–82.
[53] McMurtrie MG, Magee CL. Average volume of martensite plates during transformation. Metall Mater Trans B 1970;1(11):3185–91.

[54] Ghosh G, Raghavan V. The kinetics of isothermal martensite transformation in Fe-23.2wt%Ni-2.8wt%Mn alloy. Mater Sci Eng A 1986;80:65–74.
[55] Guimarães JRC, Rios PR. Initial nucleation kinetics of martensite transformation. J Mater Sci 2008;435:206–5210.
[56] Miyamoto G, Shibata A, Maki T, Furuhara T. Precise measurement of strain accommodation in austenite matrix surrounding martensite in ferrous alloy by electron backscatter diffraction analysis. Acta Mater 2009;57:1120–31.
[57] Shibata A, Furuhara T, Maki T. Interphase boundary structure and accommodation mechanism of lenticular martensite in Fe–Ni alloys. Acta Mater 2010;58:3477–92.
[58] Guimaraes JRC. Isothermal martensite: austenite grain size and the kinetics of 'spread'. Mater Sci Technol 2008;24: 843–7.
[59] Guimarães JRC, Gomes JC. A metallographic study of the influence of the austenite grain size on martensite kinetics in Fe-31.9Ni-0.02C. Acta Metall 1978;26:1591–6.
[60] Guimarães JRC, Rios PR. Martensite transformation intergrain and intragrain autocatalysis. Mater Res 2017;20:1548–53.
[61] Thadani NN, Meyers MA. Kinetics of martensitic transformation induced by a tensile stress pulse in Fe-31%Ni-0.035%C. Acta Metall 1986;34:1625–41.